GEOPHYSICAL RESEARCH LETTERS, VOL. 11, NO. 10, PAGES 1011-1014, OCTOBER 1984

# MEASUREMENT AND THEORY OF THE SPATIAL DISTRIBUTION OF EXCITATION BY HIGH-CURRENT ELECTRON BEAMS INJECTED INTO THE IONOSPHERE

I.L. Kofsky, D.P. Villanucci, R.B. Sluder, M.T. Chamberlain

Photometrics, Inc.

C.L. Chang, K. Ko, and K. Papadopoulos*

Science Applications, Inc.

Abstract Spatial distributions of energy deposition rates in EXCEDE Spectral's 3 keV, 7 A electron beam injection at E region altitudes derived from onboard photographic images of the air fluorescence are presented and compared with a time-dependent computational model of the collective beam-plasma interaction. The volume excitation rates decrease with a scale length of order 1 m near the rocket, are ∿2 orders of magnitude greater than predicted from single particle transport calculations, and at fixed distances from the accelerator vary by less than a factor 3 over an ambient density range of at least 40. The data are consistent with a discharge model in which the driving beam plasma instability is an absolute hydrodynamic instability with energy deposition controlled by trapping and axial dimension by ambipolar expansion of the plasma.

## Introduction

The EXCEDE Spectral artificial auroral experiment's [O'Neil et al., 1982] wide angle 16-mm cameras provided radiometrically calibrated monochrome and color photographs of the ejected electron beam between 1-1/2 m and ∿20 m from the rocket. At altitudes between ∿95 km and 128 km (apogee) the surface brightnesses have unexpectedly short decay lengths (∿1 m) [Kofsky et al., 1982]; the glow is also substantially more intense, less dependent on the ambient air density, and broader laterally than predicted from individual-electron scattering calculations [Archer, 1980].

Similar departures from linear particle beam interaction have often been observed in the ionosphere [ARAKS, 1980; Duprat et al., 1983; Grandal, Thrane, and Trøim, 1980] and low-pressure laboratory tanks [Getty and Smullen, 1963; Bernstein et al., 1979, 1983]. The effects have been attributed to the beam-plasma discharge (BPD), in which RF electrostatic waves are self-generated by a collective interaction of the charged beam with the plasma that results in avalanching [Getty and Smullin, 1963; Galeev et al., 1976; Papadopoulos, 1982]. The images from onboard EXCEDE Spectral provide the first space-resolved measurements of volume energy dissipation rates in atmospheric BPD. We present here an overview of these data and outline a time-dependent, radially-averaged computational model that is in quantitative agreement with the axial distribution of the excitation and accounts for its weak dependence on local atmospheric density.

## Experimental

EXCEDE was launched 21° E of magnetic N into a low plasma-density E region (< ∿100 R 0.3914 m aurora) at 2047 LT on 18 October 1979 from Poker Flat, Alaska. Seven amperes at 3 keV was injected in 2-sec pulses into a 30° full angle cone with axis at 60° from the rocket body. This axis was parallel to the geomagnetic field on upleg and about 4° southwest of it on downleg (always upward), so that the maximum electron pitch angle was < 20°. Two 94° x 62° -field cameras viewed from 3-1/4 m north of the accelerator, with their optic axes intercepting the beam at 4-1/2 m. (Data taken when other electron guns located closer to the cameras were operating are qualitatively similar to those reported here.) This viewing geometry is illustrated in Kofsky et al. [1982 a,b], which also show photographs and isophote plots and describe the calibration and image data reduction.

The monochrome camera (EK2475 film) was blue filtered so that when the emission spectrum is similar to that of natural aurora the exposure is ∿85% due to $N_2^+$ First Negative (0,0) and (0,1) bands at 0.3914 and 0.4278 μm and 15% to $N_2$ Second Positive bands. The color (EF7249) film showed a bluish-white (overexposed blue) "core" extending along the expected beam direction, surrounded by a weaker magenta halo (principally $N_2$ triplet-state radiations, which are selectively excited by the softer laterally-scattered secondaries). Spectra taken from onboard showed that the ratios of Second Positive to First Negative band intensities increase by only about a factor 2 above ∿100 Km (R.O'Neil, private communication, 1983). Since most (∿70%) of the active radiation from the core remains $N_2^+$ First Negative, the volume rate of ionizations of $N_2$ can be taken as proportional to the measured volume rate of this optical excitation (as in auroral investigations).

## Data

We selected for preliminary detailed analysis 0.078-sec exposures in which the only controlled experiment variable was rocket altitude (outgassing may also be varying). The operation sequence of EXCEDE's accelerators and cameras provided such data in upleg-downleg pairs at 127.8 km (apogee), 124.7 km, 122.4 km, and 118.9 km, and single downleg frames at 109.8 and 84.9 km.

*Permanent Address: University of Maryland, College Park.



Paper number 4L6193.
0094-8276/84/004L-6193$03.00

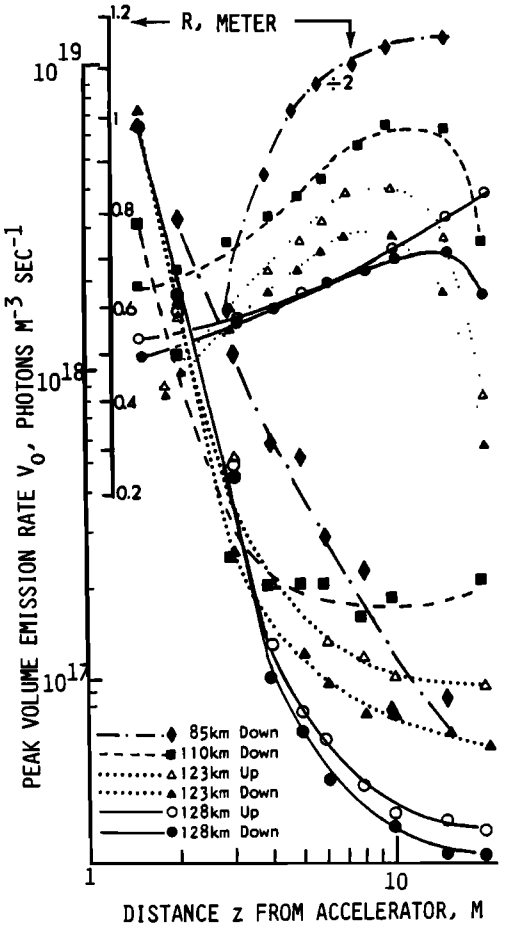


Fig. 1. Axial dependence of volume emission rate $V_o$ and width parameter R measured at four spectral altitudes.

The emission patterns' apparent cylindrical symmetry and optical thinness allows volume emission rates to be Abel-unfolded from surface radiances. The microdensitometrically-accessed transverse distributions fit gaussian functions, as evidenced by chi-squared tests. Thus the distributions can be characterized by axial volume emission rate $V_o(z)$ and width parameter R(z), where z is distance along the magnetic field line. Straightforward unfold of a gaussian radiance having maximum $B_o$ and full width to half maximum 2.354R gives $V(r) = (2\pi\sigma^2)^{-1/2} B_o \exp-(r^2/2R^2) = V_o \exp-(r^2/2R^2)$, where r is distance perpendicular to the beam axis.

The least-squares best-fit $V_o$ and R at 127.8, 122.4, 109.8, and 84.9 km are plotted in Figure 1. Except at 84.9 km $V_o(z)$ has two closely straight-line segments on the log-log plot, with its steep segment largely independent of ambient density; R at fixed z decreases slowly with altitude; and the intercept of the two-manually-drawn slopes increases very slowly with altitude, with the slope of R(z) starting to decrease at about these axial distances.

In contrast a single-particle transport model [Archer, 1980] predicts that the volume excitation rate increases slowly with z near the accelerator; it is about a factor 25 lower than measured at the z = 2 m, 122.4 km ejection altitude point. The calculated radial widths lack the maximums shown in Figure 1, and are somewhat smaller than observed near z = 4 m.

## Theoretical Model

To understand the physics of excitation rate distributions we developed a 1-D (radially averaged) time dependent model of BPD. We assume injection at altitudes of high ambient density and collisionality so that the beam-excited waves transfer their energy to electron heating rather than suprathermal tails [Papadopoulos 1982, Bernstein et al. 1983]. The plasma is treated as a fluid with density n, temperature T (thermal speed $v_e$), and fluid speed U. The basic equations (for details see Papadopoulos et al. [1983]), are

$$\frac{\partial}{\partial t} n + \frac{\partial}{\partial z} nU = N\sigma_i(v_b)v_b n_b + N\sigma_i(v_e)v_e n \quad (1a)$$

$$\frac{\partial}{\partial t} \varepsilon + \frac{\partial}{\partial z} (\varepsilon U) = Q(v_b, n_b, n, N) - \sigma_i(v_e)v_e N n \varepsilon_i - \sum_j \sigma_j(v_e)v_e N n \varepsilon_j \quad (1b)$$

$$\frac{\partial}{\partial t}\Gamma + \frac{\partial}{\partial z} (\Gamma U) = -\frac{1}{2}\frac{\partial}{\partial z}\left(\frac{nT}{M}\right) . \quad (1c)$$

Here $\varepsilon = n(mU^2/2 + 3T/2)$, $\Gamma = nU$, m(M) the electron (ion) mass, $\sigma_i$ and $\varepsilon_i$ the ionization cross section and mean energy loss, and $\sigma_j$ and $\varepsilon_j$ the excitation cross sections and energy losses (taken from Green and Stolarski [1972]) of neutral species of local density N. $n_b$ and $v_b$ are the beam density and velocity, and $Q(v_b, n_b, n, N)$ is a term that describes the rate and functional dependence of electron heating due to the beam plasma instability (BPI). Note that the zero dimensional description of the interaction requires only the particle conservation and energy rate equations (1a, 1b), while for axially resolved BPD profiles the momentum equation (1c) is also needed.

A relatively simple prescription was adopted for Q, which is based on stabilization by trapping of an absolute BPI [Seidl et al., 1976]:

$$Q = [1-\exp(-n/n_c)] \cdot \alpha n_b E_b v_b S(z-L)/L. \quad (2)$$

The first term in Eq. (2) is a switch-on term for BPI, with $n_c$ the density required for triggering; $\alpha = (n_b/n)^{1/3}$ is the efficiency of transfer of beam energy $E_b$ within an interaction volume of axial length L, which we took as the feedback oscillator length $2\pi v_b \alpha^{-1} \omega_e^{-1}$; S(z-L) is a step function; and $\omega_e$ is the electron plasma frequency. The details of the plasma physics involved appear elsewhere [Papadopoulos, 1984].

Calculated axial dependences of n, T and the 0.3914 $\mu$m emission for an injection altitude of 122-1/2 km ($N \approx 8 \times 10^{11}$ $cm^{-3}$) at 10 msec after start of beam injection into a flux tube are shown in Figure 2. The model results are in reasonably good agreement with both the observed relative axial profile and numerical values of volume emission rate. Figure 3 shows the axial variation $V_o$

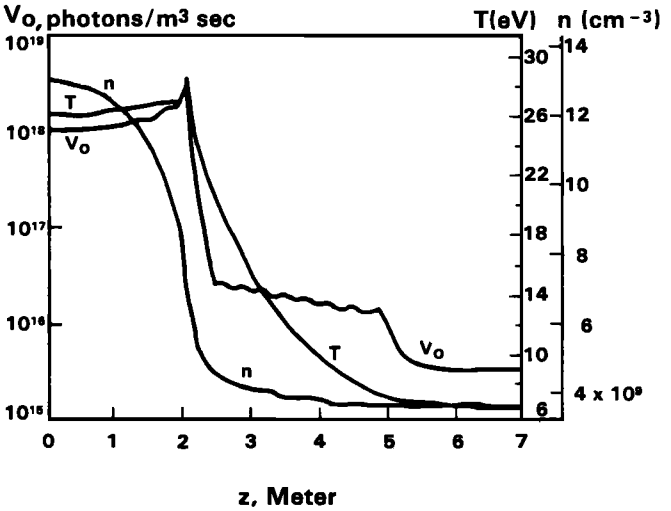


Fig. 2. Computed axial dependence of density n, temperature T and emission rate $V_o$ at 10 msec after initial beam injection, for an injection altitude of 123 km.

at the altitudes in Figure 1. Notice that the profile becomes less sharp at higher altitude, with some evidence of the increase in length of the strongly-emitting region that would be inferred from the crossover of about-linear segments. This can be explained by examining the electron temperature, which controls the rate of expansion of the heated plasma. At low altitudes excitation of air species is increasingly important relative to ionization, reducing the plasma pressure nT for a specific energy deposition. This results in a weaker expansion force $\partial nT/\partial z$ and a sharper excitation profile. (The limited spatial resolution of our computational grid exaggerates the steepness of the profile at 110 and 95 km altitude.)

Interesting conclusions about spatially-averaged BPD scaling can be found by axially averaging Eq. (1). Assuming $\partial\Gamma/\partial t = 0$, $T >> MU^2$, and neglecting heat losses ($\partial\varepsilon U/\partial z = 0$), we find

$$\frac{\partial n}{\partial t} = \sigma_j(v_b)v_b N n_b + \sigma_i(v_e)v_e N n - \frac{nC_s}{L} \quad (3a)$$

$$\frac{3}{2}\frac{\partial T}{\partial t} = \frac{Q}{n} - \frac{3}{2}\frac{1}{n}\frac{\partial n}{\partial t}T - \sigma_i(v_e)v_e N\varepsilon_i - \sum_j \sigma_j(v_e)v_e N\varepsilon_j \quad (3b)$$

where $C_s$ is the ion sound speed. The steady state values from the numerical solution of Eq. (3) are shown as a function of injection altitude in Figure 4. Note that steady state BPD occurs at the higher altitudes ($T > 15\text{-}1/2$ eV, the ionization potential of $N_2$), but not at 95 km ($N \approx 10^{13}$ cm$^{-3}$) where $T \approx 6$ eV and only transient BPD is achieved. The averaged 0.3914 μm volume excitation rate at any z varies by less than a factor 3 over a factor-40 range in neutral density, in semiquantitative accord with the results in Figure 1; the change in electron temperature (i.e., mean impact excitation cross section) is in the direction compensating the change in N. While a BPI occurs at all altitudes, the high electron density due to beam ionization when $N \approx 10^{13}$ reduces the heating efficiency of the BPI so that no avalanche is produced by the plasma electrons (i.e., the second term on the right side of Eq. (3a) goes to zero).

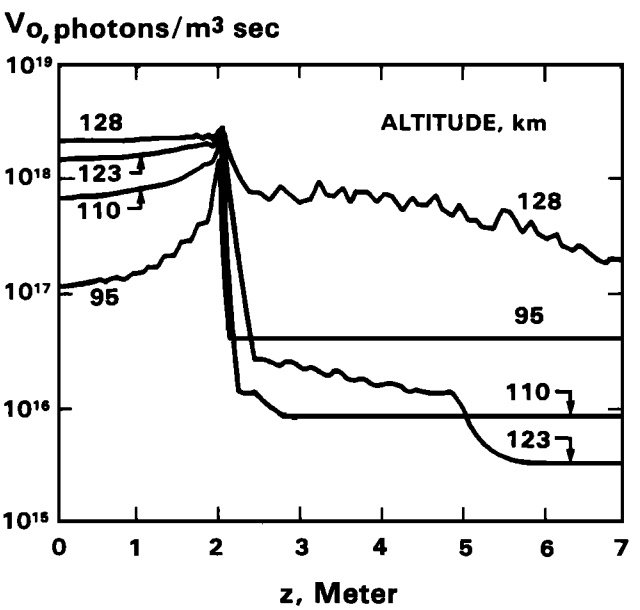


Fig. 3. Computed emission rate $V_o$ as a function of axial distance z at four injection altitudes.

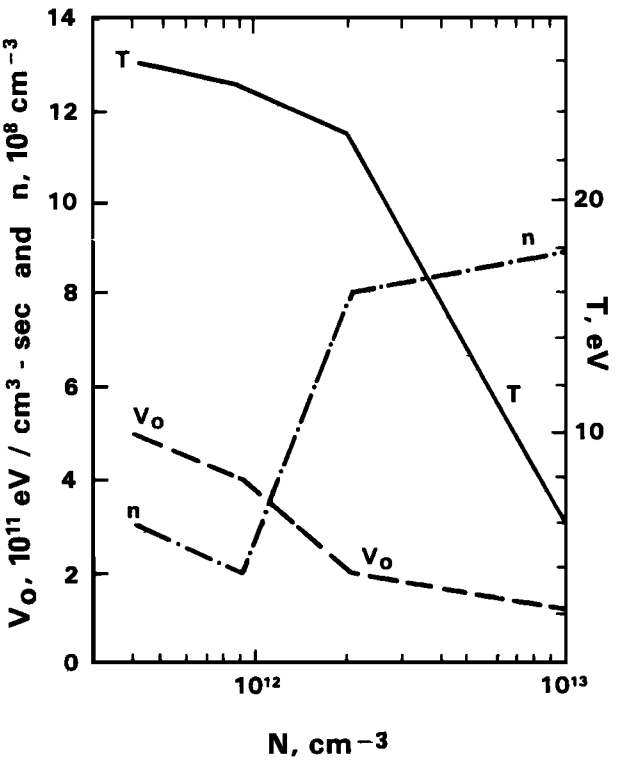


Fig. 4. Steady state values of density n, temperature T and emission rate $V_o$ from numerical solution of Eq. (3).

## Summary and Conclusions

We presented the first spatially resolved measurements of volume luminosity caused by electron beam injection in the ionosphere. Previous measurements with low spatial resolution indicated the need for short length energy deposition which could be attributed to BPI. The sharp energy deposition gradients (1-2 m) of Figure 1 require physics considerations past simple BPI. Notice that even if the energy deposition due to BPI occurs at "zero" length, i.e. the localization of Q in Eq. (2) is $\delta(z)$, the observed deposition length will be of the order of $L_d \approx v_e/\nu_{en} >> (5 \times 10^{13}/N)$m (N is neutral density in $cm^{-3}$, $\nu_{en}$ is the electron-neutral collision frequency) for 100 eV electrons. At 123 km ($N \approx 8 \times 10^{11}$) this will give $L_d >> 60$ m. The resolution of this dilemma is the electron confinement required by quasi-neutrality and incorporated in Eq. (1c). The effective expansion velocity of the electrons is not $v_e$, as in conventional single particle models, but the sound speed $C_s = v_e(m/M)^{1/2}$. Therefore the deposition length is $L_d \approx v_e(m/M)^{1/2}/\nu_{en}$ which for 123 km with the computed $T \approx 25$ eV gives $L_d \approx 1$-2 m. For the energy deposition length due to BPI to be shorter or comparable to $L_d$ an absolute instability (i.e. oscillator behavior) is required, as discussed in Papadopoulos [1984].

Quasineutrality and oscillator behavior are the key physical considerations in our theoretical model, which, given the approximations made in Eqs. (1), agrees remarkably well with the observed emission gradients, excitation rates, and altitude scaling. To reiterate, only the combination of short energy deposition lengths such as expected in absolute instabilities and axial electron confinement can produce the measured emission gradients. More complete models with non-Maxwellian electrons, accurate dependence axial deposition, and radial dependence will be presented elsewhere.

These findings apply to energetic beam injection from space shuttle, in that the presence of regions of high neutral density ($N \approx 10^{11} - 10^{13}$ $cm^{-3}$) surrounding the spacecraft and expanding to distances of at least 2m might be sufficient to trigger BPD.

Acknowledgments. Work supported by DNA 001-81-C-0003 and 001-83-C-0128. The authors appreciate the help of W. McKechney of DNA, and R. O'Neil of AFGL and A. Drobot of SAI in many aspects of the work.

## References

ARAKS special issue, Ann. Geophys., 36 No. 3, 1980.

Archer, D.H., Excede energy deposition: Theory and experiment compared, Rep. DNA 5525F, AD-A102522, 62 pp., Defense Nuclear Agency Washington, D.C., 30 Nov 1980.

Bernstein, W., H. Leinbach, P.J. Kellogg, S.J. Monson, and T. Hallinan, Further laboratory measurements of the beam plasma discharge, J. Geophys. Res., 84, 7271-7278, 1979.

Bernstein, W., J.O. McGarity, and A. Konradi, Electron beam injection experiments: Replication of flight observations in a laboratory beam plasma discharge, Geophys. Res. Lett., 10, 1124-1127, 1983.

Duprat, G.R.J., B.A. Whalen, A.G. McNamara, and W. Bernstein, Measurements of the stability of energetic electron beams in the ionosphere, J. Geophys. Res., 88, 3095-3108, 1983.

Galeev, A.A., E.V. Mishin, R.Z. Sagdeev, V.D. Shapiro, and V.I. Shevchenko, Discharge in the region around a rocket following injection of electron beams into the ionosphere, Soy. Phys. Dokl., 21, 641-643, 1976.

Getty, W.D., and L.D. Smullin, Beam-plasma discharge: Buildup of oscillations, J. Appl. Phys., 34, 3421-3429, 1963.

Grandal, B., E.V. Thrane, and J. Trøim, Polar 5: An electron accelerator experiment within an aurora: 4. Measurements of 391.4 nm light produced by an artificial electron beam in the upper atmosphere, Planet. Space Sci., 28, 309-319, 1980.

Green, A.E.S. and R. Stolarski, Analytic models of electron impact excitation cross-sections, J. Atm. Terr. Phys., 34, 1703-1717, 1972.

Kofsky, I.L., R. B. Sluder, and D.P. Villanucci, Onboard radiometric photography of EXCEDE Spectral's ejected electron beam, in Artificial Particle Beams in Space Plasma Studies, edited by B. Grandal, pp. 217-228, Plenum, New York, 1982a.

Kofsky, I.L., M.T. Chamberlain, and D.P. Villanucci, Interpretation of EXCEDE Spectral and auroral infrared simulation data, Rep. DNA-TR-81-191, AD-A137267, 96 pp., Defense Nuclear Agency Washington, D.C., 30 Nov. 1982b.

O'Neil, R.R., A.T. Stair, Jr., W.R. Pendleton, Jr., and D. Burt, The EXCEDE Spectral artificial auroral experiment: An overview in Artificial Particle Beams in Space Plasma Studies, edited by B. Grandal, pp. 207-215, Plenum, New York, 1982.

Papadopoulos, K., Theory of beam plasma discharge, in Artificial Particle Beam in Space Plasma Studies, edited by B. Grandal, pp. 505-523, Plenum, New York, 1982.

Papadopoulos, K., C.L. Chang, and K. Ko, Collective plasma effects on electron beam injection from rockets, Rep. SAI-83-1215, 62 pp., Science Applications, Inc., McLean, VA, 1983.

Papadopoulos, K., On the plasma physics of the beam plasma discharge, Comments in Plasma Physics, in press 1984.

Seidl, M., W. Carr, D. Boyd, and R. Jones, Nonlinear development of absolute and convective instabilities, Phys. Fluids, 19, 78-92, 1976.

M.T. Chamberlain, I.L. Kofsky, R.B. Sluder, and D.P. Villanucci, Photometrics, Inc., Woburn, MA 01801

C.L. Chang, K. Ko, and K. Papadopoulos, Science Applications, Inc., McLean, VA 22102

(Received June 11, 1984;
accepted July 2, 1984.)